Reprogramming of endogenous Müller cells into photoreceptor-like cells induced by small-molecule compounds in mice

Yuya Fujii
Kyushu University Graduate School of Medical Sciences
Mitsuru Arima (m-arima@eye.med.kyushu-u.ac.jp)
Kyushu University Graduate School of Medical Sciences
Yusuke Murakami
Kyushu University Graduate School of Medical Sciences
Koh-Hei Sonoda
Kyushu University Graduate School of Medical Sciences

Article

Keywords: Müller cells (MCs), RNA of rhodopsin (Rho), age-related macular degeneration (AMD), retinitis pigmentosa (RP)

Posted Date: September 17th, 2021

DOI: https://doi.org/10.21203/rs.3.rs-890527/v1

Article

Reprogramming of endogenous Müller cells into photoreceptor-like cells induced by small-molecule compounds in mice

Yuya Fujii,[1] Mitsuru Arima,[*1,2] Yusuke Murakami,[1] Koh-Hei Sonoda[1]

[1]Department of Ophthalmology, Graduate School of Medical Sciences, Kyushu University, Fukuoka, Japan

[2]Center for Clinical and Translational Research, Kyushu University Hospital, Fukuoka, Japan

***Corresponding author**: Mitsuru Arima

Department of Ophthalmology, Graduate School of Medical Sciences, Kyushu University, 3-1-1 Maidashi, Higashi-ku, Fukuoka City, Fukuoka, Japan

Tel: +81-92-642-5648, Fax: +81-92-642-5663.

Email: m-arima@eye.med.kyushu-u.ac.jp

Abstract

Lifelong visual impairment occurs from retinal diseases due to the inability of photoreceptor cells to regenerate in mammals. We demonstrated that endogenous Müller cells (MCs) in mice differentiate into photoreceptor-like cells by intravitreal injection of four small-molecule compounds: tumor growth factor-β inhibitor, bone morphogenetic protein inhibitor, glycogen synthase kinase 3 inhibitor, and γ-secretase inhibitor. *In vitro*, the messenger RNA of rhodopsin (Rho) in MCs increased 30-fold, and 25% of cultured MCs expressed Rho protein 7 days after stimulation with these compounds. *In vivo*, Rho-positive cells were regenerated on day 7 after the intravitreal injection of four compounds, accompanied with recovery of Rho-derived scotopic function. Lineage tracing in mice treated with N-methyl-N-nitrosourea, a disease model of photoreceptor degeneration, showed that the regenerated Rho-positive cells were originated from endogenous MCs. Finally, the regeneration of Rho-positive cells was also induced in the retina of rd10 mice, a model with similar genetic mutation as humans. Notably, the intravitreal injection significantly reduced cone cell death in rd10 mice. This treatment could be a new strategy in retinal regenerative medicine where mammalian endogenous MCs are reprogrammed into photoreceptor cells independent of transplantation or gene transfer.

Introduction

Various retinal diseases damage photoreceptor cells, leading to irreversible visual dysfunction[1,2]. There are many researches in this decade on induced pluripotent stem cell transplantation and gene therapy to treat the visual dysfunction of retinitis pigmentosa (RP) and age-related macular degeneration (AMD) that are typical retinal degenerative diseases[3–5]. The results of these preclinical and clinical studies revealed that stem cell therapy[6] and viral gene transfer[7] are effective in restoring vision. However, these therapies have disadvantages, namely, the high cost of developing and manufacturing cellular medicine; the risk of complications such as immune rejection and tumorigenesis; and the need for special techniques for transplanting cells/cell sheets and vectors[8].

In central nerve regeneration, it has been reported that the administration of small-molecule compounds enables reprogramming into neurons and neural progenitor cells[9–11]. Mahato et al. showed that fibroblasts could differentiate into retinal progenitor cells[12]. Zhang et al. confirmed that endogenous astrocytes differentiate into neurons in mice injected with inhibitors into their ventricles[13]. These reports served as motivations to explore the possibility of differentiation of retinal component cells (i.e., endogenous cells) into photoreceptor cells following the administration of compounds.

Retinal glial cells are composed of Müller cells (MCs), astrocytes, and microglia[14]. In zebrafish, MCs have been shown to be a source of new photoreceptor cells after retinal injury[15]. Unfortunately, mammalian MCs do not possess the ability to generate new photoreceptor cells. However, Ueki et al.[16] and Jorstad et al.[17] reported that MCs could be reprogrammed into retinal neurons in mice by gene transfer of Ascl1; this gene is essential for photoreceptor regeneration in zebrafish, similar to high mobility group A1 (HMGA1)[18]. Additionally, Yao et al. showed MC-derived rod cell production by gene transfer of β-catenin, Otx2, Crx, and Nr l[19]. Based on the findings of previous researches, we hypothesized that it might be possible to produce MC-derived photoreceptors by stimulation with small-molecule compounds.

In the present study, we demonstrated that the administration of four compounds (SB431542, LDN193189, CHIR99021, and DAPT) could reprogram mouse MCs into rhodopsin (Rho)-positive cells *in vitro* and *in vivo*. We showed that intravitreal injection of these compounds induced the differentiation of endogenous MCs into Rho-positive cells in mice treated with N-methyl-N-nitrosourea (MNU) and in rd10 mice; these are disease models of retinal degeneration. Along with the regeneration of Rho-positive cells, the a-wave of the

electroretinogram (ERG) was restored, suggesting that Rho-positive cells had properties similar to those of rod cells.

In retinal diseases such as RP and AMD, irreversible damage to photoreceptor cells progresses gradually[2, 20]. Unlike cell transplantation and gene therapy, intravitreal injection of compounds is inexpensive and easy to re-perform, and it may be applicable to patients at various stages of the disease.

Results

Screening of small-molecule compounds for converting MCs to photoreceptor cells.

We isolated MCs from 6-week-old B6J mice, according to previous reports (Supplementary Fig. 1)[21]. We examined the changes in the expression of photoreceptor markers and transcription factors in primary MCs after stimulation with candidate compounds to test whether the compounds could chemically reprogram MCs into photoreceptor cells.

We selected five compounds that act on signaling pathways important for neural differentiation; these have been used in multiple studies[9,10,13,22–26]. The selection is based on previous reports on the successful differentiation of somatic cells, including fibroblasts and

astrocytes, into neurons by small-molecule compounds. The compounds used were the following: SB431542 (tumor growth factor-β [TGF-β] inhibitor), LDN193189 (bone morphogenetic protein [BMP] inhibitor), CHIR99021 (glycogen synthase kinase-3β [GSK-3β] inhibitor), DAPT (γ-secretase inhibitor), and Y-27632 (ROCK inhibitor).

The time course of *the in vitro* experiments is shown in Fig. 1a. First, the expression of photoreceptor markers was examined by polymerase chain reaction (PCR) analysis 7 days after stimulation with all 31 combinations of the five compounds (Fig. 1b). The expression level of the messenger RNA (mRNA) of opsin (cone cell marker) was below detection sensitivity in all combinations. On one hand, the expression level of Rho (rod cell marker) mRNA was markedly increased to about 30-fold of the control in the combination of SB431542, LDN193189, CHIR99021, and DAPT (Fig. 1*B*). Immunocytochemistry showed that these four compounds induced the expression of Rho protein in 25% of living cells (Fig. 1c, d). The expression levels of genes regulated by these inhibitors were also evaluated. Compound stimulation increased the expression of Axin2 (a downstream molecule of the Wnt/β-catenin pathway) and decreased the expression of LTBP1 (a downstream molecule of TGF-β pathway), Id (a downstream molecule of BMP pathway), and DLL1 (a downstream molecule of Notch pathway), suggesting that the signaling pathways corresponding to each

compound were inhibited (Supplementary Fig. 2).

The morphology of the MCs gradually changed from day 4, and a neurite-like structure was observed on day 7 (Fig. 1e). The expression of CD44, an MC marker[27], significantly decreased with the change in cell morphology (Fig. 1f). We found that Ascl1 expression peaked on day 1. HMGA1, which is essential for the regeneration of photoreceptor cells in zebrafish[16,18], was significantly upregulated after stimulation (Supplementary Fig. 3). We also confirmed increased expression of SOX2, a retinal progenitor marker[28], 1 day after stimulation with the four compounds (Supplementary Fig. 3). In addition, we quantified the expression of retinal neuron markers other than Rho, but none of them increased (Fig. 1g). This phenomenon of increased Rho expression and decreased expression of glial cell markers was observed not only in primary mouse cells, but also in rat cell lines (Fig. 1h). These results suggest that MCs can be differentiated into rod-like cells by the simultaneous administration of the four compounds.

Ectopic expression of Rho in wild-type mice by intravitreal injection of compounds.

Based on the *in vitro* results, we explored the possibility that simultaneous administration of these four compounds by intravitreal injection may lead to the differentiation of endogenous

MCs into rod cells. The *in vivo* experimental protocol is shown in Fig. 2a. Six-week-old wild-type B6J mice (WT mice) received intravitreal injection every 3 days, and Rho expression in the retina was assessed on days 3, 7, and 14 by immunohistochemistry (IHC) and PCR. The layered structure of the retina is shown in Fig. 2b. Although there was no difference in Rho expression in the outer retina between the compound-stimulated and control groups on days 7 and 14, ectopic Rho expression in the outer plexiform layer (OPL) was detected in the compound-stimulated group (Fig. 2c). The mRNA expression levels of retinal neuron-specific markers, including Rho, in the whole retina did not differ between the two groups (Fig. 2d and Supplementary Fig. 4a). To confirm the induction of Rho expression in MCs by four-compound stimulation, CD44+ CD45- cells were purified from retinas by magnetic-activated cell separation, and Rho mRNA in these cells was quantified by PCR. As shown in Fig. 2e, a significant increase in Rho expression was observed in the compound-stimulated group. It is also noteworthy that there was no increase in other neural markers, except for Rho, in CD44+ CD45- cells (Fig. 2f). The upregulation of Rho expression was only observed on day 3 and may be due to the decrease in the expression of CD44 as MCs differentiated into Rho-positive cells. ERGs showed no clear difference in amplitude of a-wave, b-wave, or oscillatory potential between the control and compound-stimulated groups, and there was no evidence that the newly produced Rho-positive cells functioned as neurons (Supplementary Fig. 4b).

Why was the expression of Rho in WT mice only "ectopic"? Unlike mammals, zebrafish can regenerate the retina. Retinal regeneration occurs when retinal progenitor cells, generated by the migration and division of MCs activated by injury, differentiate into different types of neurons[29]. Ueki et al. reported that overexpression of Ascl1 in MCs causes MCs to differentiate into retinal neurons such as amacrine cells, bipolar cells, and photoreceptor cells, but this regenerative response does not occur without retinal damage[16]. These reports suggest that retinal injury forms a "niche" suitable for regeneration. In addition, adherens junctions and tight junctions are well developed in the outer limiting membrane (OLM), and the permeability of cells and substances is strictly controlled[30]. This barrier may prevent the newly born Rho-positive cells from extending their cell bodies between the OLM and retinal pigment epithelium (RPE).

Thus, we hypothesized that injury to the outer retinal layer would create an environment suitable for photoreceptor regeneration. In this study, we used two models of retinal degeneration to confirm the possibility that the four compounds could induce MCs to differentiate into photoreceptor cells.

Induction of Rho expression in the outer retina and restoration of retinal function in MNU-treated mice.

First, we used a model of chemical retinal degeneration induced by MNU, that has a potent carcinogen, teratogen, and mutagen[31]. MNU damages the outer retinal layers, such as the RPE layer, outer nuclear layer (ONL), and OPL, while causing little damage to the inner retinal layers. MNU induces progressive photoreceptor apoptosis, RPE degeneration, and subretinal fibrosis; it has been widely used in research to elucidate the pathogenesis of RP and AMD[32]. Furthermore, MNU promotes MC hypertrophy and upregulates the expression of glial fibrillary acidic protein (GFAP), a stress marker in MCs that may create an "injury-induced niche" suitable for MCs to differentiate into photoreceptor cells.

We determined the dose of MNU at which the ONL disappeared 7 days after intraperitoneal injection (Supplementary Fig. 5). We then performed intravitreal injections of the four compounds on days 0, 3, and 6 after administration of 75 mg/kg MNU to investigate whether photoreceptor regeneration occurred in the outer retinal layer (Fig. 3a). The IHC results are shown in Fig. 3b. Peanut agglutinin (PNA) that selectively binds to the cone inner and outer segments, did not differ between the control and compound-stimulated groups; however, Rho expression was significantly increased in the compound-stimulated group (Fig. 3b, c).

Quantification of the percentage of Rho-expressing retinal region in the total retinal length showed that Rho expression was significantly higher after intravitreal injection of the four compounds (Fig. 3d).

We then tested whether the difference in the expression of Rho-positive cells between the control and compound-stimulated groups depended on cell regeneration or on the inhibition of cell apoptosis. PCR showed a significant increase in Rho mRNA only on day 7 after the administration of four compounds (Fig. 3e and Supplementary Fig. 6), but there was no difference in the number of apoptotic cells (Fig. 3f, g), suggesting that new Rho-positive cells may have been produced.

We used a lineage-tracing model that expressed the td-Tomato protein to track MCs, for confirmation that the Rho-positive cells originated from MCs. PAAV.GFAP.Cre.WPRE.hGH, which is an adeno-associated virus (AAV) containing human GFAP promoter, was injected into the vitreous of 2-week-old ROSA-td-Tomato mice so that MCs could be visualized. Four weeks after injection into the vitreous, IHC showed that td-Tomato co-localized with glutamine synthetase, indicating the introduction of AAV into MCs (Supplementary Fig. 7). On day 7 after MNU administration, td-Tomato was co-expressed with Rho in the outer retinal

layer, suggesting that Rho-positive cells originated from MCs (Fig. 3h). Fluorescent-activated cell sorting (FACS) results showed that treatment with the compounds increased the expression level of Rho, but did not change the expression levels of other neural markers in Tomato-positive cells (Fig 3i). These results were consistent with those obtained in primary cells and WT mice, suggesting that td-Tomato-positive MCs were reprogrammed to rods or rod-like cells, not to other retinal neurons, by the four compounds administered. Postsynaptic density protein 95 (PSD95), a synaptic marker, was also expressed around newly produced Rho-positive cells in the OPL of the retina (Fig. 3j).

Next, to evaluate whether the four compounds could restore retinal dysfunction, ERGs were recorded 7 days after the four compounds were injected into MNU-treated mice. In mice treated with 75 mg/kg MNU, the four compounds increased Rho expression in IHC (Fig 3b), but there was no obvious improvement in ERG (Fig 4a). Since the ERG waveform disappeared after the 75 mg/kg MNU administration, it was possible that the retinal dysfunction might have been so severe that the effect of the four compounds could not be detected. Therefore, the dose was reduced to 30 mg/kg and ERG was performed again. As shown in Fig. 4a and 4b, the amplitude of the a-waves was significantly improved by the injection of the four compounds. These findings suggest that Rho-positive cells induced by

simultaneous administration of the four compounds to the vitreous restored retinal dysfunction in MNU-treated mice.

Induction of Rho expression in the outer retina and inhibition of cone cell death in rd10 mice. Finally, we tested the retinal regenerative capacity of these four compounds in rd10 mice, a mouse model of RP with a missense point mutation in the β-subunit of the rod cyclic guanosine monophosphate phosphodiesterase gene (PDE6β)[33]. Point mutations of *PDE6β* have been detected in patients with autosomal recessive RP[34]. In rd10 mice, rod cell death peaked at 3–4 weeks, followed by cone cell death[35]. We then performed intravitreal injections of the four compounds every 3 days in 4-week-old rd10 mice and investigated the changes in Rho expression (Fig. 5a). We first quantified the expression of retinal neuron markers in the whole retina using PCR. After treatment with the four compounds, only the expression of Rho was upregulated, and the expression levels of other markers remained unchanged. (Fig. 5b and Supplementary Fig. 8). Moreover, IHC showed an obvious increase in Rho expression in the outer retina of the compound-stimulated group (Fig. 5c, d). We quantified the percentage of Rho-expressing retinal region in the total retinal length; indeed, Rho expression was significantly increased by intravitreal injection of the four compounds (Fig. 5e).

It is known that rod cell death is followed by cone cell death in RP, but the cause of cone cell death is not clearly understood. In addition to the oxidative stress caused by excessive oxygen accumulation in the outer retinal layer due to rod cell death and the release of toxic substances from damaged rod cells[33,36], Léveillard et al. and Mohand-Said et al. reported that a decrease in the secretion of survival factors from rods is the cause of cone cell death[37,38]. Byrne et al. have shown that cone cell death can be suppressed by gene transfer of the rod-derived cone viability factor (RdCVF) encoded by nucleoredoxin-like 1 (NXNL1)[39].

Next, we counted PNA-positive cone cells based on our previous report[33] to verify the inhibition of cone cell death associated with increased expression of Rho-positive cells. Retinal whole-mount staining showed that significantly more PNA-positive cone cells were retained on day 7 after intraocular injection of the four compounds (Fig. 5f, g). In addition, the expression of NXNL1 was significantly increased in the compound-stimulated group (Fig. 5h), suggesting that the newly produced Rho-positive cells may secrete RdCVF.

Discussion

In this study, we reprogrammed MCs into Rho-positive cells both i*n vitro* and *in vivo*. These

Rho-positive cells can improve retinal function in a model of retinal degeneration. It should be emphasized that endogenous cells in the retina were only differentiated into photoreceptor-like cells through the simultaneous administration of the four compounds.

In WT and MNU-treated mice, we found that MCs were reprogrammed into Rho-positive cells after reverting to progenitor cells by stimulation with the four compounds. MC-driven Rho-positive cells did not show elevated expression of other retinal neural markers, suggesting that MCs could only be induced into rod or rod-like cells. In zebrafish, MC-derived progenitor cells have the ability to differentiate into various types of neurons, but they generate unneeded neurons because of their multipotency[40]. Ueki et al. also reported that MCs overexpressing Ascl1 differentiate not only into photoreceptor cells, but also into amacrine and bipolar cells[16]. If these compounds can be administered to cause MCs to differentiate only into rods or rod-like cells, this therapy will have an advantage over other therapies in terms of safety. MCs play an important role in supporting the function, metabolism, and structure of neurons in the retina. In other words, if MCs are depleted by inducing MCs into nerves, abnormalities in retinal function may occur. However, in this study, there was no obvious abnormality in the retinal layer structure or loss of function due to compound administration. MCs are capable of asymmetric self-renewal after injury[41,42]; therefore, no

obvious depletion may have occurred.

This treatment strategy is also valuable in real-world clinical applications. Advances in omics analysis are rapidly revealing the signaling pathways required for neural regeneration. Although still in the preclinical stage, it is now possible to differentiate non-neuronal cells into retinal neurons or retinal progenitor cells by modifying specific signaling pathways through genome editing with virus vectors or compound stimulation. If autologous transplantation is possible, concerns about rejection will be alleviated. However, the development of gene therapy and cell therapy products is costly. Therefore, we decided to investigate the possibility of direct differentiation of retinal endogenous cells into photoreceptor cells using molecular compounds that can be made inexpensively; these compounds have the potential for mass production. From an ophthalmologist's perspective, we also wanted to make the treatment as simple as possible. It has been reported that different signals are required for different stages of neural differentiation, but we wanted to achieve retinal regeneration with a single mixture of molecular compounds.

In the mammalian retina, unlike in the central nervous system, there are no reports of neural regeneration solely by direct reprogramming using compounds. However, the signaling

pathways that are modified by the compounds used in this study have also been shown to be important in retinal regeneration. Osakada et al. demonstrated that activation of Wnt/β-catenin signaling by GSK-3β inhibitors promotes the proliferation of MC-derived retinal progenitors after injury[43]. Lenkowski et al.[44] and Todd et al.4[5] reported that the TGFb-Smad2/3 signaling pathway regulates the regeneration of retinal neurons after injury in zebrafish. They showed that the inhibition of this pathway suppresses MC-derived gliosis and induces proliferation of MC-derived progenitor cells. In addition, Ueki et al. showed that the activated BMP-Smad1/5/8 signaling pathway promotes MC-derived gliosis in proliferative vitreoretinopathy[46]. Moreover, DAPT increased the expression of Crx, which is important for rod photoreceptor maturation and promotes photoreceptor differentiation. Therefore, we speculate that CHIR99021, a Wnt/β-catenin activator, SB431542, a TGF-β inhibitor, and LDN193189, a BMP inhibitor, may lead to the proliferation of MC-derived neural progenitor cells and DAPT. A notch inhibitor may contribute to the differentiation toward rod photoreceptors.

In vitro results showed that simultaneous administration of these four compounds increased the efficiency of Rho-positive cell production. We confirmed that each targeted signaling pathway was properly inhibited, even when four compounds were administered

simultaneously. The number of Rho-positive cells decreased in the absence of any of the four compounds and with the addition of an extra compound. These results suggest that the suppression of TGF, BMP, and Notch signaling pathways and the activation of the Wnt/β-catenin signaling pathway may have created an environment suitable for the regeneration of rod or rod-like cells. In the present study, the efficiency of differentiation of primary MCs into Rho-positive cells was only 25%. Single-cell analysis[47,48] has shown that there is diversity in MCs, and it is possible that some types are more likely to differentiate into Rho-positive cells upon stimulation with compounds. In addition, in most previous reports, when multiple compounds were used to increase the efficiency of differentiation of non-neuronal cells into neuronal cells, the timing of administration of each compound was changed. When multiple compounds were administered simultaneously, as in the present study, it may have been difficult to strictly control the signals.

It was also possible to suppress the apoptosis of cone cells in rd10 mice; this reveals a clinical application of the intravitreal injection of these compounds. The rods are sensitive enough to detect a single photon and are suitable for night vision. However, rods rarely function in bright areas because they are saturated by moderately bright light. On the other hand, the cones are 100 times less sensitive to light than the rods, so they do not function in the dark. However,

the cones have an excellent ability to adjust their sensitivity, so they do not saturate even in bright areas. Generally, visual acuity and color vision depend on the function of the cones[36]. This study suggests that the secretion of RdCVF from MC-derived Rho-positive cells may inhibit the death of cone cells. If the cone cells of RP patients can be maintained, the quality of vision will be improved. The rate of degeneration is slower in human RP as compared to rd10 mice, allowing more time for therapeutic intervention and the ability to treat more patients.

The limitation of this study is that the two mouse models, MNU-treated mice and rd10 mice, do not fully reflect human RP and AMD. MNU treatment results in the destruction of the outer retinal layer in approximately one week. In other words, there is a difference between the phenomena that occur in the retinas of MNU-treated mice and those of slowly progressing human RP and AMD. In addition, although rd10 mice have the same mutation as in humans, the same results may not be obtained for all types of RP because more than 100 different causative genes have been reported in human RP. In addition, once-every-three-day intravitreal injections cannot be used in clinical practice. Appropriate dosages and intervals must be established using drug delivery systems or developing extended-release agents.

In this study, we showed that the simultaneous administration of four compounds alone can differentiate retinal MCs into Rho-positive cells and restore the function of the injured retina. This method can be applied not only to RP and AMD, but also to photoreceptor degeneration caused by various retinal diseases. Vitreous injection of the compound is expected to be a new strategy for retinal regeneration therapy that does not rely on cell transplantation or gene transfer.

Methods

Animals. *Male and female* B6 wild-type (WT) mice, B6.Cg-Gt(ROSA)26Sortm14(CAG-tdTomato)Hze/J (ROSA-td-Tomato) mice, and B6.CXB1-Pde6βrd10/J (rd10) mice were used. ROSA-td-Tomato and rd10 mice were purchased from the Jackson Laboratory. To perform the experiments, mice were anesthetized by intraperitoneal injection of 15 mg/kg ketamine and 7 mg/kg xylazine. The chemical-induced retinal degeneration model was created by intraperitoneal administration of a single dose of MNU in mice. After anesthesia, the mice were weighed, and MNU was injected (30–75 mg/kg). All mice were treated in accordance with the standards of the Association for Research in Vision and Ophthalmology for the use of animals in ophthalmic and vision research. All animal experiments were reviewed and approved by the Kyushu University Ethics Committee for Animal Experimentation and were

conducted in accordance with the relevant guidelines and regulations (A20-360, A21-225).

Cell culture. Primary retinal MCs were cultured as previously described[21]. Briefly, the eyes of 6-week-old WT mice were enucleated under sterile conditions. Isolated retinas were then digested with collagenase D (1.2 mg/mL, Roche, Mannheim, Germany) and DNAse I (0.005%, Roche). Cells were seeded onto a Poly L-Lysine-coated dish (Corning, NY, USA) and cultured at 34 °C in 5% CO_2. The culture medium (CM) was composed of DMEM high glucose (Sigma-Aldrich, St Louis, MO, USA), 0.1% penicillin-streptomycin, and 10% fetal bovine serum. The rat MC cell line (TR-MUL5) was purchased from Fact, Inc. (Sendai, Japan), and cultured in the same culture medium.

Stimulation with small-molecule compounds in MCs and TR-MUL5 cells in vitro. One day before administration of the compounds, half of the culture medium was replaced with the stimulating medium composed of Ham's F-12 (FUJIFILM Wako, Osaka, Japan), N2 supplement (Thermo, Waltham, MA, USA), and 0.1% penicillin-streptomycin. The next day, all of the medium was replaced with stimulating medium. Five compounds, namely, SB431542 (5 μM, Nacalai, Kyoto, Japan), LDN193189 (1 μM, R&D Systems, Minneapolis, MN, USA), CHIR99021 (1.5 μM Cayman, Ann Arbor, MI, USA), DAPT (5 μM, Sigma-Aldrich),

and Y-27632 (0.5 μM, Nacalai) were added to the SM. The medium was changed every two days and the compounds were added at the same time.

Intravitreal injection. After anesthesia, the compounds were injected into the vitreous of 6-week-old WT, ROSA-td-Tomato, and 2-and 4-week-old rd10 mice under topical mydriasis. The final concentrations of SB431542, LDN193189, CHIR99021, and DAPT were 0.1 μM, 0.02 μM, 0.03, and 0.1 μM, respectively. Micro syringes with 33-gauge needles (Hamilton, Reno, NV, USA) were used. After anesthesia, we injected intravitreally of 1 μl pAAV.GFAP.Cre.WPRE.hGH, with a concentration was 7 x 10^{13} vg/μL, to 2-week-old ROSA-td-Tomato mice. PAAV.GFAP.Cre.WPRE.hGH was a gift from James M. Wilson (Addgene plasmid # 105550 ; http://n2t.net/addgene:105550 ; RRID:Addgene_105550).

Quantitative real-time PCR (qPCR). Total RNA of retinal tissue and cultured cells was extracted using the NucleoSpin RNA Kit (Macherey-Nagel, Düren, Germany) according to the manufacturer's instructions. RNA was reverse transcribed using the First Strand cDNA Synthesis Kit for RT-PCR (Roche). Real-time qPCR was performed using SYBR Premix Ex Taq (Takara, Shiga, Japan) with a LightCycler 96 (Roche). The primer sequences used are listed in Supplementary Table 1.

Immunocytochemistry. Cultured cells were fixed with 4% paraformaldehyde at room temperature for 20 min. After washing with phosphate buffered saline (PBS), cells were incubated with 0.3% Triton-X 100 (FUJIFILM Wako) in PBS for 15 min and blocked with PBS containing 10% normal goat serum (NGS) (Thermo) for 1 h at room temperature. Cells were then incubated with primary antibodies (chicken anti-vimentin [ab24525, Abcam, Cambridge, UK], rabbit anti-glutamine synthetase [GS] [ab73593, Abcam], mouse anti–rhodopsin [1D4, Abcam], and rat anti-mouse CD44-PE [1M7, eBioscience, San Diego, CA, USA]) at 4°C overnight. Next, the cells were incubated with Alexa-conjugated secondary antibodies (Thermo) for 1 h at room temperature, and the nuclei were counterstained with 4′,6-diamidino-2-phenylindole (DAPI). Immunofluorescence images were acquired using a BZ-X710 microscope (Keyence, Osaka, Japan). For cell counting, at least three locations (fields) were selected per dish.

Immunohistochemistry (frozen section). Eyes were enucleated, fixed with 4% paraformaldehyde for 30 min at room temperature, and immersed in OCT compound. Frozen sections were cut with a cryostat (CM1800, Leica Microsystems, Wetzlar, Germany) at 8 μm and mounted onto MAS-coated glass slides (MAS-01, Matsunami, Osaka, Japan). After

removing the OCT compound in PBS containing 0.3% Triton X-100 for 15 min, sections were blocked with 10% NGS in PBS for 1 h. Sections were then incubated with primary antibodies (chicken anti-vimentin [ab24525, Abcam], mouse anti–rhodopsin [1D4, Abcam], FITC-conjugated PNA [L7381, Sigma-Aldrich], rabbit anti-PSD95 [D27E11, Cell Signaling Technology, Danvers, MA, USA], rabbit anti-GS [ab73593, Abcam]) at 4°C overnight. After washing with PBS, the sections were incubated with Alexa-conjugated secondary antibody for 1 h at room temperature, and the nuclei were counterstained with DAPI.

Immunohistochemistry (paraffin section). After fixation with 4% paraformaldehyde for 30 min at room temperature, the eyes of mice were embedded in paraffin and sliced into 3-μm sections. After removal of the paraffin, the sections were activated, blocked, and incubated with primary antibodies (chicken anti-vimentin [ab24525, Abcam], mouse anti–rhodopsin [1D4, Abcam], FITC-conjugated PNA [L7381, Sigma-Aldrich], rabbit anti-PSD95 [D27E11, Cell Signaling Technology, rabbit anti-GS [ab73593, Abcam]) at 4 °C overnight. After washing with PBS, the sections were incubated with Alexa-conjugated secondary antibody for 1 h at room temperature, and the nuclei were counterstained with DAPI. Images were acquired using a BZ-X710 microscope (Keyence). Rho-positive length in the outer retinal layers was analyzed using ImageJ software. At least three sections, including the optic nerve, were

measured per eye, and the average was calculated.

Fluorescent activated cell sorting (FACS). For flow cytometry measurements, cultured cells were washed with PBS, 0.25% trypsin was added, and the cells were incubated for 3 min at 37°C. After washing with 2% bovine serum albumin (BSA) in PBS, the cells were fixed with 1% paraformaldehyde and permeabilized in 0.3% Triton X-100 for 10 min at 4°C. After rinsing, the cells were incubated with an antibody (rat anti-Vimentin-APC [IC2105A, R&D Systems], rat anti CD44-PE [eBioscience]) for 1 h at 4°C. After rinsing, the cells were resuspended in 2% BSA in PBS and analyzed by FACS. FACSVerse and FlowJo software (BD Biosciences, Franklin Lakes, NJ, USA) were used for the analysis. For td-Tomato-positive cell sorting, isolated retinas from ROSA-td-Tomato mice were incubated with collagenase D (1.2 mg/ml) and DNAse I (0.005%) for 20 min at 37°C. After washing with 2% BSA in PBS, the cells were stained with 7-Amino-Actinomycin D Viability Staining Solution (BioLegend, San Diego, CA, USA) to remove dead cells. A BD FACSAria™ III cell sorter (BD Biosciences) was used for live td-Tomato-positive cell sorting.

TUNEL staining. TUNEL staining was performed using an ApopTag Fluorescein In Situ Apoptosis Detection Kit (Merck Millipore, Darmstadt, Germany) according to the

manufacturer's instructions. The number of TUNEL-positive cells in the ONL was counted as described for MNU-treated mice[49]. Briefly, the number of TUNEL-positive cells in the ONL of a 9000 (150 × 60) μm^2 area, each 400 μm away from the optic nerve papilla and ciliary body, were counted in a masked fashion. Then, we calculated the average number of TUNEL-positive cells in four areas per section.

Retinal whole-mount staining. Eyes were enucleated and fixed with 4% paraformaldehyde for 1 h at 4°C. The isolated retinas were incubated with PBS containing 0.5% Triton-X 100 for 30 min and blocked for 1 h with PBS containing 10% NGS and 0.5% Triton-X 100. The retinas were then incubated with FITC-conjugated PNA (L7381, Sigma-Aldrich) at 4°C overnight. After washing with PBS, the retinas were mounted on slides. To assess the number of cone photoreceptor cells, we counted the PNA-positive cells in 125 × 125 μm^2 retinal areas in the superior, inferior, temporal, and nasal areas located 250 μm, 500 μm, and 1,000 μm from the optic disc. The names and conditions of the samples were masked by the observers. The number of PNA-positive cells was averaged from 12 retinal areas in each retina.

Immunofluorescence images were acquired using a BZ-X710 microscope (Keyence).

Electroretinograms. ERGs were recorded as described in detail[50]. Briefly, mice were dark-adapted overnight and anesthetized under dim red light. After mydriasis, recordings were made using the PuREC system (Mayo, Aichi, Japan), as previously reported[51]. ERGs were recorded on day 7 after intravitreal injections of the four compounds, according to the International Society for Clinical Electrophysiology of Vision standard protocol with five light stimuli per recording. The scotopic ERGs were elicited using a stimulus intensity of 10 000 cd m^{-2}. The responses were differentially amplified and filtered between 0.3 and 500 Hz.

Statistics and reproducibility. Data are presented as the mean ± standard error of mean (SEM). Statistical analysis was performed using JMP Pro version 16.0 (SAS Institute). The significance of the difference was determined using two-tailed Student's *t*-test. Differences were considered statistically significant at $P < 0.05$. The number of biological repeats (n) for each experiment is noted in the figure legends.

References

1. Busskamp, V., Picaud, S., Sahel, J. A., & Roska, B. Optogenetic therapy for retinitis pigmentosa. *Gene Ther*. **19**, 169-175 (2012).

2. Hartong, D. T., Berson, E. L., & Dryja, T. P. Retinitis pigmentosa. *Lancet* **368**, 1795-1809 (2006).

3. Kuriyan, A. E. et al. Vision Loss after Intravitreal Injection of Autologous "Stem Cells" for AMD. *N. Engl. J. Med*. **376**, 1047-1053 (2017).

4. Mazzilli, J. L. et al. A preclinical safety study of human embryonic stem cell-derived retinal pigment epithelial cells for macular degeneration. *J. Ocul. Pharmacol. Ther*. **36**, 65–69 (2020).

5. Sanges, D. et al. Reprogramming Müller glia via in vivo cell fusion regenerates murine photoreceptors. *J. Clin. Invest*. **126**, 3104–3116 (2016).

6. Mandai, M. et al. Autologous induced stem-cell-derived retinal cells for macular degeneration. *N. Engl. J. Med*. **376**, 1038–1046 (2017).

7. Cehajic-Kapetanovic, J. et al. Initial results from a first-in-human gene therapy trial on X-linked retinitis pigmentosa caused by mutations in RPGR. *Nat. Med*. **26**, 354–359 (2020).

8. Wright, L. S. et al. Induced pluripotent stem cells as custom therapeutics for retinal repair: progress and rationale. *Exp. Eye Res*. **123**, 161-172 (2014).

9. Hu, W. et al. Direct conversion of normal and Alzheimer's disease human fibroblasts into

neuronal cells by small molecules. *Cell Stem Cell*. **17**, 204–212 (2015).

10. Li, X. et al. Small-molecule-driven direct reprogramming of mouse fibroblasts into functional neurons. *Cell Stem Cell*. **17**, 195–203 (2015).

11. Cheng, L. et al. Generation of neural progenitor cells by chemical cocktails and hypoxia. *Cell Res.* **25**, 645-646 (2015).

12. Mahato, B. et al. Pharmacologic fibroblast reprogramming into photoreceptors restores vision. *Nature* **581**, 83–88 (2020).

13. Zhang, L. et al. Small molecules efficiently reprogram human astroglial cells into functional neurons. *Cell Stem Cell*. **17**, 735–747 (2015).

14. Vecino, E. et al. Glia-neuron interactions in the mammalian retina. *Prog. Retin. Eye Res*. **51**, 1–40 (2016).

15. Goldman D. Müller glial cell reprogramming and retina regeneration. *Nat. Rev. Neurosci*. **15**, 431–442 (2014).

16. Ueki, Y. et al. Transgenic expression of the proneural transcription factor Ascl1 in Müller glia stimulates retinal regeneration in young mice. *PNAS* **112**, 13717–13722 (2015).

17. Jorstad, N. L. et al. Stimulation of functional neuronal regeneration from Müller glia in adult mice. *Nature* **548**, 103–107 (2017).

18. Hoang, T. et al. Gene regulatory networks controlling vertebrate retinal regeneration.

Science **370**, eabb8598 (2020).

19. Yao, K. et al. Restoration of vision after de novo genesis of rod photoreceptors in mammalian retinas. *Nature* **560**, 484–488 (2018).

20. Curcio, C. A., Medeiros, N. E., & Millican, C. L. Photoreceptor loss in age-related macular degeneration. *Invest. Ophthalmol. Vis. Sci*. **37**, 1236–1249 (1996).

21. Hicks, D., & Courtois, Y. The growth and behaviour of rat retinal Müller cells in vitro. 1. An improved method for isolation and culture. *Exp. Eye Res*. **51**, 119–129 (1990).

22. Dai, P., Harada, Y., & Takamatsu, T. Highly efficient direct conversion of human fibroblasts to neuronal cells by chemical compounds. *J. Clin. Biochem. Nutr*. **56**, 166–170 (2015).

23. Shi, Y. et al. Induction of pluripotent stem cells from mouse embryonic fibroblasts by Oct4 and Klf4 with small-molecule compounds. *Cell Stem Cell*. **3**, 568–574 (2008).

24. Wang, Y. et al. Chemical conversion of mouse fibroblasts into functional dopaminergic neurons. *Exp. Cell Res*. **347**, 283–292 (2016).

25. Cheng, L. et al. Direct conversion of astrocytes into neuronal cells by drug cocktail. *Cell Res*. **25**, 1269–1272 (2015).

26. Gao, L. et al. Direct generation of human neuronal cells from adult astrocytes by small molecules. *Stem Cell Reports* **8**, 538–547 (2017).

27. Wang, H. et al. Short hairpin RNA-mediated knockdown of VEGFA in Müller cells reduces

intravitreal neovascularization in a rat model of retinopathy of prematurity. *Am. J. Pathol*. **183**, 964–974 (2013).

28. Taranova, O. V. et al. SOX2 is a dose-dependent regulator of retinal neural progenitor competence. *Genes Dev*. **20**, 1187–1202 (2006).

29. Wan, J., & Goldman, D. Retina regeneration in zebrafish. *Curr. Opin. Genet. Dev*. **40**, 41–47 (2016).

30. Omri, S. et al. The outer limiting membrane (OLM) revisited: clinical implications. *Clin. Ophthalmol*. **4**, 183–195 (2010).

31. Tsubura, A., Yoshizawa, K., Kuwata, M., & Uehara, N. Animal models for retinitis pigmentosa induced by MNU; disease progression, mechanisms and therapeutic trials. *Histol. Histopathol*. **25**, 933–944 (2010).

32. Chen, Y., Luo, X., Liu, S., & Shen, Y. Neuroprotective effect of cannabinoid receptor 1 antagonist in the MNU-induced retinal degeneration model. *Exp. Eye Res*. **167**, 145–151 (2018).

33. Nakatake, S. et al. MUTYH promotes oxidative microglial activation and inherited retinal degeneration. *JCI Insight* **1**, e87781 (2016).

34. McLaughlin, M. E., Sandberg, M. A., Berson, E. L., & Dryja, T. P. Recessive mutations in the gene encoding the β–subunit of rod phosphodiesterase in patients with retinitis

pigmentosa. *Nat. Genet*. **4**, 130–134 (1993).

35. Kanan, Y. et al. Metipranolol promotes structure and function of retinal photoreceptors in the rd10 mouse model of human retinitis pigmentosa. *J. Neurochem.* **148**, 307–318 (2019).

36. Campochiaro, P. A., & Mir, T. A. The mechanism of cone cell death in retinitis pigmentosa. *Prog. Retin. Eye Res*. **62**, 24–37 (2018).

37. Léveillard, T. et al. Identification and characterization of rod-derived cone viability factor. *Nat. Genet*. **36**, 755–759 (2004).

38. Mohand-Said, S. et al. Normal retina releases a diffusible factor stimulating cone survival in the retinal degeneration mouse. *PNAS* **95**, 8357–8362 (1998).

39. Byrne, L. C. et al. Viral-mediated RdCVF and RdCVFL expression protects cone and rod photoreceptors in retinal degeneration. *J. Clin. Invest*. **125**, 105–116 (2015).

40. Powell, C. et al. Zebrafish Müller glia-derived progenitors are multipotent, exhibit proliferative biases and regenerate excess neurons. *Sci. Rep*. **6**, 24851 (2016).

41. Kassen, S. C. et al. Time course analysis of gene expression during light-induced photoreceptor cell death and regeneration in albino zebrafish. *Dev. Neurobiol*. **67**, 1009–1031 (2007).

42. Nagashima, M., Barthel, L. K., & Raymond, P. A. A self-renewing division of zebrafish Müller glial cells generates neuronal progenitors that require N-cadherin to regenerate retinal

neurons. *Development* **140**, 4510–4521 (2013).

43. Osakada, F. et al. Wnt signaling promotes regeneration in the retina of adult mammals. *J. Neurosci*. **27**, 4210–4219 (2007).

44. Lenkowski, J. R. et al. Retinal regeneration in adult zebrafish requires regulation of TGFβ signaling. *Glia* **61**, 1687–1697 (2013).

45. Todd, L. et al. BMP- and TGFβ-signaling regulate the formation of Müller glia-derived progenitor cells in the avian retina. *Glia* **65**, 1640–1655 (2017).

46. Ueki, Y., & Reh, T. A. EGF stimulates Müller glial proliferation via a BMP-dependent mechanism. *Glia* **61**, 778–789 (2013).

47. Hu, F. Y. et al. Cell development deficiency and gene expression dysregulation of trisomy 21 retina revealed by single-nucleus RNA sequencing. *Front. Bioeng. Biotechnol*. **8**, 564057 (2020).

48. Menon, M. et al. Single-cell transcriptomic atlas of the human retina identifies cell types associated with age-related macular degeneration. *Nat. Commun*. **10**, 4902 (2019).

49. Yoshizawa, K. et al. Caspase-3 inhibitor rescues N-methyl-N-nitrosourea-induced retinal degeneration in Sprague-Dawley rats. *Exp. Eye Res*. 71, 629–635 (2000).

50. Tanimoto, N. et al. Vision tests in the mouse: Functional phenotyping with electroretinography. *Front. Biosci.* (Landmark Ed.) **14**, 2730–2737 (2009).

51. Nakama, T. et al. Inhibition of choroidal fibrovascular membrane formation by new class of RNA interference therapeutic agent targeting periostin. *Gene Ther*. **22**, 127–137 (2015).

Acknowledgements

The authors thank Iori Wada, Mitsuhiro Kurata, Masayo Eto, and Fumiyo Morikawa (Kyushu University) for technical assistance. This study was supported by JSPS KAKENHI with grant numbers JP18H02956 and JP21H03094, given to KH Sonoda. Research funding was from Senju Pharmaceutical Co., Ltd., given to M Arima, Y Murakami, and KH Sonnoda. The funders had no role in the study design, data collection and analysis, decision to publish, or preparation of the manuscript. The authors also thank Editage (www.editage.com) for English language editing.

Author contributions

M Arima designed this study with Y Fujii. Critical assistance was provided by Y Murakami and KH Sonoda. Y Fujii and M Arima performed the *in vitro* and *in vivo* experiments and data analysis. Y Fujii and M Arima wrote the manuscript. All the authors approved the final version of the manuscript.

Competing Interests

The authors have declared that no conflict of interest exists.

Figure Legends

Figure 1. Screening of small-molecule compounds for converting primary MCs to photoreceptor-like cells.

a Time course of *in vitro* experiments. MCs were stimulated with four compounds every 2 days. S, SB431542 (5 μM); L, LDN193189 (1 μM); C, CHIR99021 (1.5 μM); D, DAPT (5 μM); Y, Y-27632 (0.5 μM). **b** Comparison of Rho mRNA expression levels in all 31 combinations using real time qPCR. In the four-compound (SB431542, LDN193189, CHIR99021, DAPT) group, the expression increased about 30-fold compared to the dimethyl sulfoxide (DMSO) group. n = 3. **c** and **d** Immunofluorescence of Rho (**c**) and the corresponding quantitative results (**d**) on day 7 after stimulation with the four compounds. **c** Rho expression increased after the stimulation with four compounds. Scale bar = 100μm. **d** The percentage of Rho positive cells significantly increased after the administration of four compounds. n = 3. **e** Microscopic images of cultured cells. A neurite-like structure could be observed on day 7 after the stimulation with four compounds. Scale bar = 100 μm. **f** Real time qPCR results of retinal cell-specific markers and CD44 on day 7 after the stimulation with four compounds. Rho expression significantly increased and CD44 expression significantly decreased by the administration of four compounds. n = 3. **g** Real time qPCR results of Rho and glutamine synthetase (GS) expression in TR-MUL5. Rho expression significantly increased on day 1

and 3, and GS expression significantly decreased on day 5 after the stimulation with four compounds. n = 3 DMSO group; n = 5 compound group.

All data are presented as the mean ± SEM. *P < 0.05, **P < 0.01, Student's t-test.

Figure 2. Ectopic expression of Rho in WT mice by intravitreal injection of four compounds.

a Time course of *in vivo* experiments using WT mice. Four compounds were intravitreally injected every 3 days. **b** Hematoxylin and eosin staining of mouse retina. INL, inner nuclear layer; OPL, outer plexiform layer; ONL, outer nuclear layer; OLM, outer limiting membrane; RPE, retinal pigment epithelium. **c** Immunohistochemistry of vimentin (green) and Rho (red) on day 7 and 14 after intravitreal injection of compounds. Ectopic Rho (yellow arrows) in OPL appeared after the injection of compounds. Vim, vimentin. Scale bar = 100 μm. **d** Real-time qPCR results of Rho expression. There was no significant change in the level of Rho mRNA in the whole retina (n = 4), but it was significantly increased in CD44+ CD45- cells. n = 6. **e** Real-time qPCR results of retinal neuron specific markers in CD44+ CD45- cells. n = 6. All data are presented as the mean ± SEM, *P < 0.05, Student's t-test.

Figure 3. Reprograming of MCs into Rho-positive cells in MNU-treated mice.

a Time course of *in vivo* experiments using MNU-treated mice. After a single systemic administration of 75 mg/kg MNU, intravitreal injection of four compounds was performed every 3 days. i.p., intraperitoneal injection; TUNEL, TdT-mediated dUTP nick end labeling. **b** Immunohistochemistry of Rho (yellow arrows) on day 3 and 7 after intravitreal injection of compounds in MNU-treated mice. Scale bar = 400 μm. **c** Magnified images of Rho (red) and PNA (green) expression in (**b**). The compound group showed increased Rho expression in the outer retinal layer. Scale bar = 100 μm. **d** Quantitative results of percentages of Rho-expressing retinal region in the total retinal length (**b**). Rho-expressing retinal region was significantly longer in the compound group. n = 3. **e** Real-time qPCR results of Opsin and Rho expression from the whole retina on day 7 after intravitreal injection of compounds. Rho expression was significantly increased by four compounds. n = 4. **f** and **g** TUNEL staining (**f**) and quantification of TUNEL-positive photoreceptor cells (**g**) on day 3 after intravitreal injection of compounds. There is no difference in photoreceptor cell death between the two groups. n = 3. Scale bar = 100 μm. **h** Td-Tomato (red) was co-expressed with Rho (green) in the outer retinal layer on day 7 after intravitreal injection of compounds in MNU-treated GFAP-td-Tomato mice. Scale bar = 50 μm. **i** Real-time qPCR results of Rho expression and other retinal neuron-specific markers from td-Tomato-positive cell population on day 7 after intravitreal injection. Rho expression was significantly increased by four compounds. n = 3. **j**

PSD95 (white) was also expressed around Rho-positive cells in the OPL. Scale bar = 20 μm. All data are presented as the mean ± SEM. *P < 0.05, **P < 0.01, Student's t-test.

Figure 4. Improvement of retinal function by MC-derived Rho-positive cells.

a Scotopic responses of ERGs on day 7 after intravitreal injection of four compounds. ERG waveforms for the 75 mg/kg MNU group are shown in red, and those for the 30 mg/kg MNU group are shown in blue. **b** Effect of compounds on the a-wave in the 30 mg/kg MNU group. The amplitude of the a-waves was significantly improved by compounds. All data are mean ± SEM. n = 4, *P < 0.05, Student's t-test.

Figure 5. Contribution of Rho-positive cells to the suppression of cone cell death in rd10 mice.

a Time course of *in vivo* experiments using rd10 mice. Intravitreal injection of four compounds was performed every 3 days for 2 weeks from 4 weeks of age. **b** Real time qPCR results of Opsin and Rho expression from whole retina on day 7 after intravitreal injection of compounds. Rho expression significantly increased by four compounds. n = 4. **c** and **d** Immunohistochemistry of Rho (**c**) and quantitative results of percentages of Rho-expressing retinal region in the total retinal length (**d**) on day 14 after intravitreal injection of compounds.

Rho expression was clearly increased in the compound group. Scale bar = 200 μm. n = 4. **e** Magnified images of Rho (red) expression and bright field (BF) in (**c**). Scale bar = 100 μm. **f** and **g** Whole-mount PNA staining (**f**) and quantification of PNA-positive cone cells (**g**) in the outer retinas on day 7 after intravitreal injection of 4 compounds. n = 3, Scale bar = 50 μm. **h** Real-time qPCR result of NXNL1 on day 7 after intravitreal injection of 4 compounds. NXNL1 expression was significantly increased by four compounds. n = 4. All data are presented as the mean ± SEM. *$P < 0.05$, Student's *t*-test.

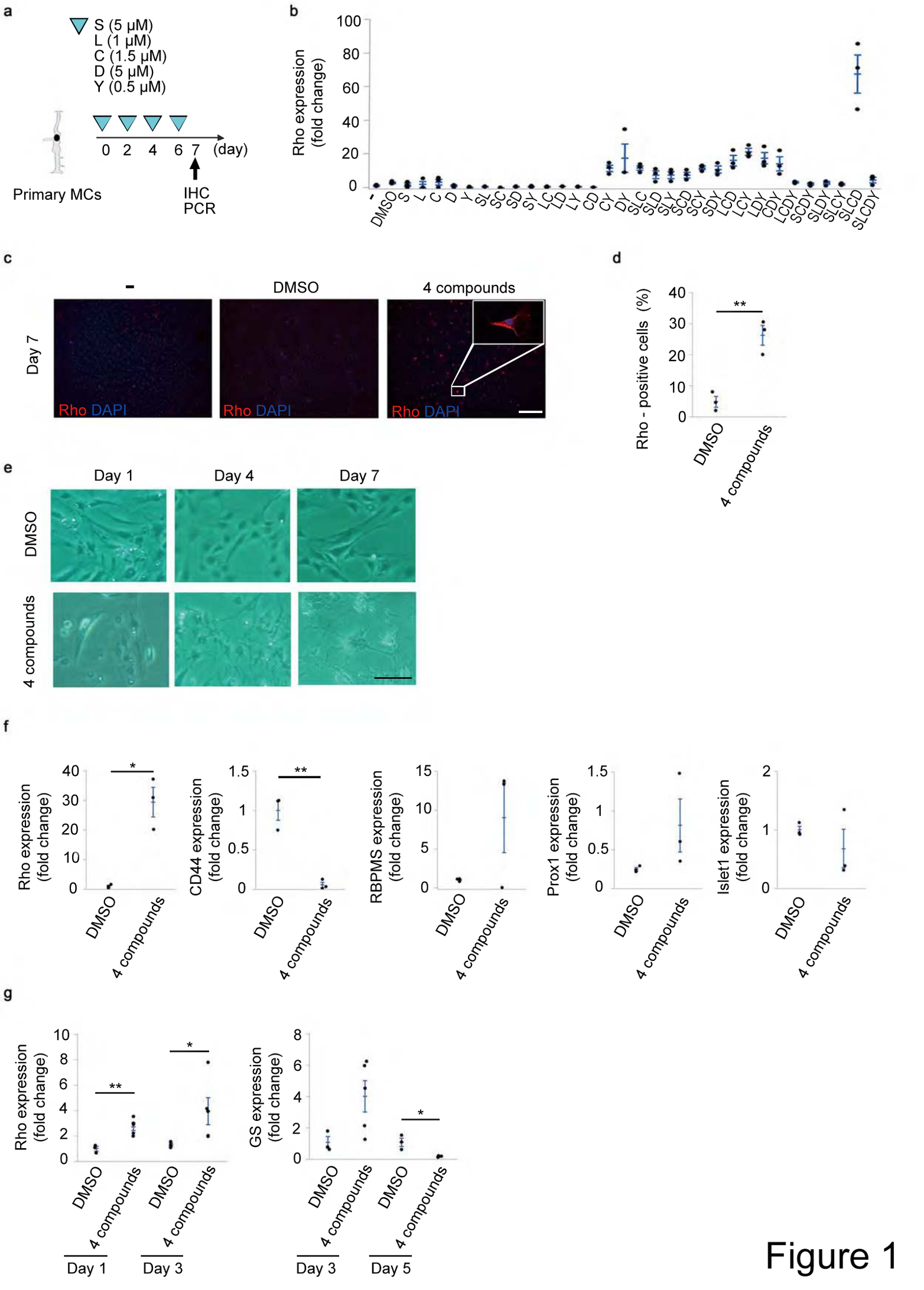
a
S (5 μM)
L (1 μM)
C (1.5 μM)
D (5 μM)
Y (0.5 μM)
0 2 4 6 7 (day)
Primary MCs
IHC
PCR
b
Rho expression (fold change)
100
80
60
40
20
0
-
DMSO
S
L
C
D
Y
SL
SC
SD
SY
LC
LD
LY
CD
CY
DY
SLC
SLD
SLY
SCD
SCY
SDY
LCD
LCY
LDY
CDY
LCDY
SCDY
SLDY
SLCY
SLCD
SLCDY
c
-
DMSO
4 compounds
Day 7
Rho DAPI
Rho DAPI
Rho DAPI
d
Rho - positive cells (%)
40
30
20
10
0
**
DMSO
4 compounds
e
Day 1
Day 4
Day 7
DMSO
4 compounds
f
Rho expression (fold change)
40
30
20
10
0
*
DMSO
4 compounds
CD44 expression (fold change)
1.5
1
0.5
0
**
DMSO
4 compounds
RBPMS expression (fold change)
15
10
5
0
DMSO
4 compounds
Prox1 expression (fold change)
1.5
1
0.5
0
DMSO
4 compounds
Islet1 expression (fold change)
2
1
0
DMSO
4 compounds
g
Rho expression (fold change)
10
8
6
4
2
0
**
*
DMSO
4 compounds
DMSO
4 compounds
Day 1
Day 3
GS expression (fold change)
8
6
4
2
0
*
DMSO
4 compounds
DMSO
4 compounds
Day 3
Day 5

Figure 1

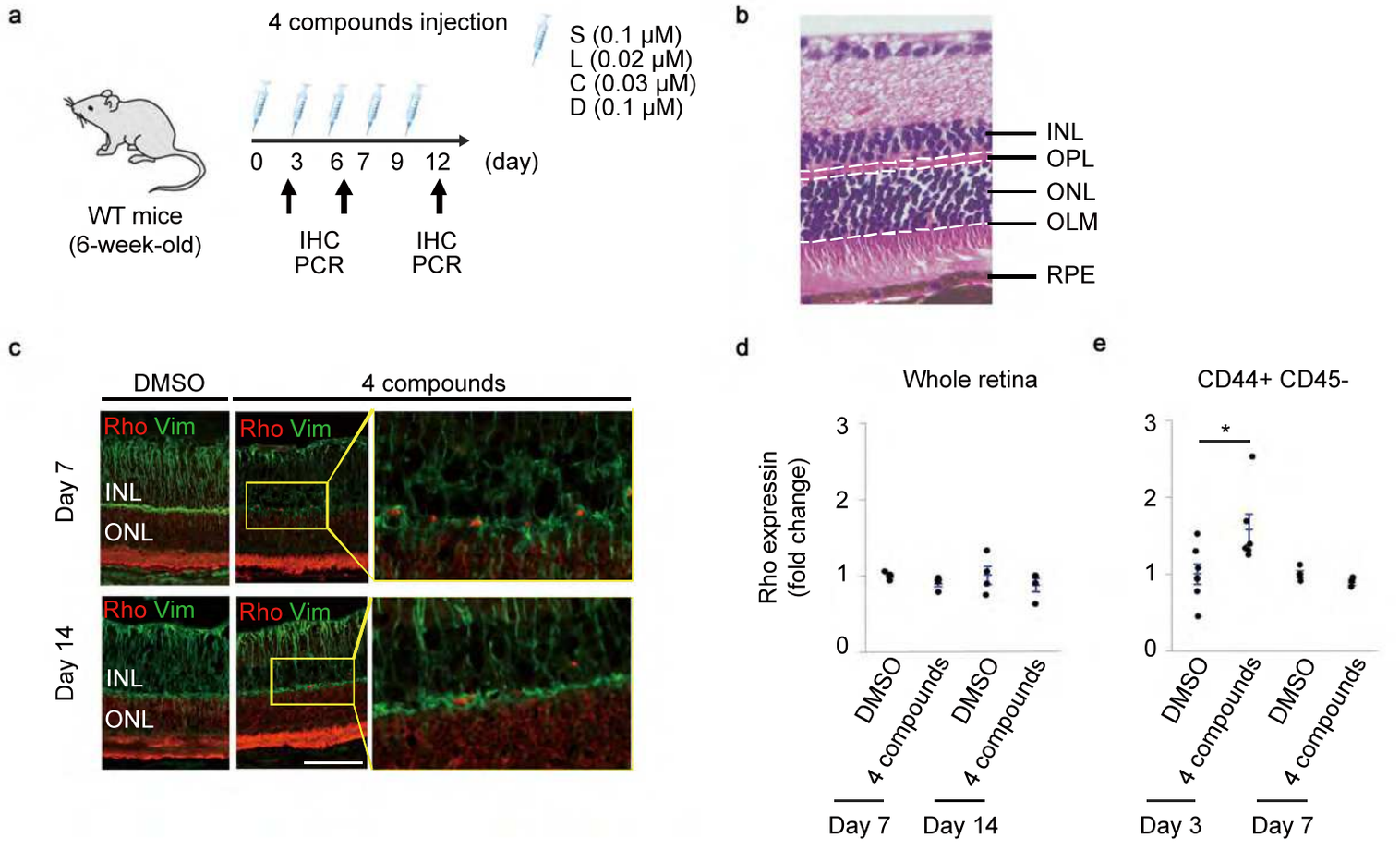
a
4 compounds injection
S (0.1 μM)
L (0.02 μM)
C (0.03 μM)
D (0.1 μM)
WT mice
(6-week-old)
0 3 6 7 9 12 (day)
IHC
PCR
IHC
PCR
b
INL
OPL
ONL
OLM
RPE
c
DMSO
4 compounds
Day 7
Day 14
Rho Vim
INL
ONL
d
Whole retina
Rho expressin
(fold change)
DMSO
4 compounds
Day 7
Day 14
e
CD44+ CD45-
*
Day 3
Day 7

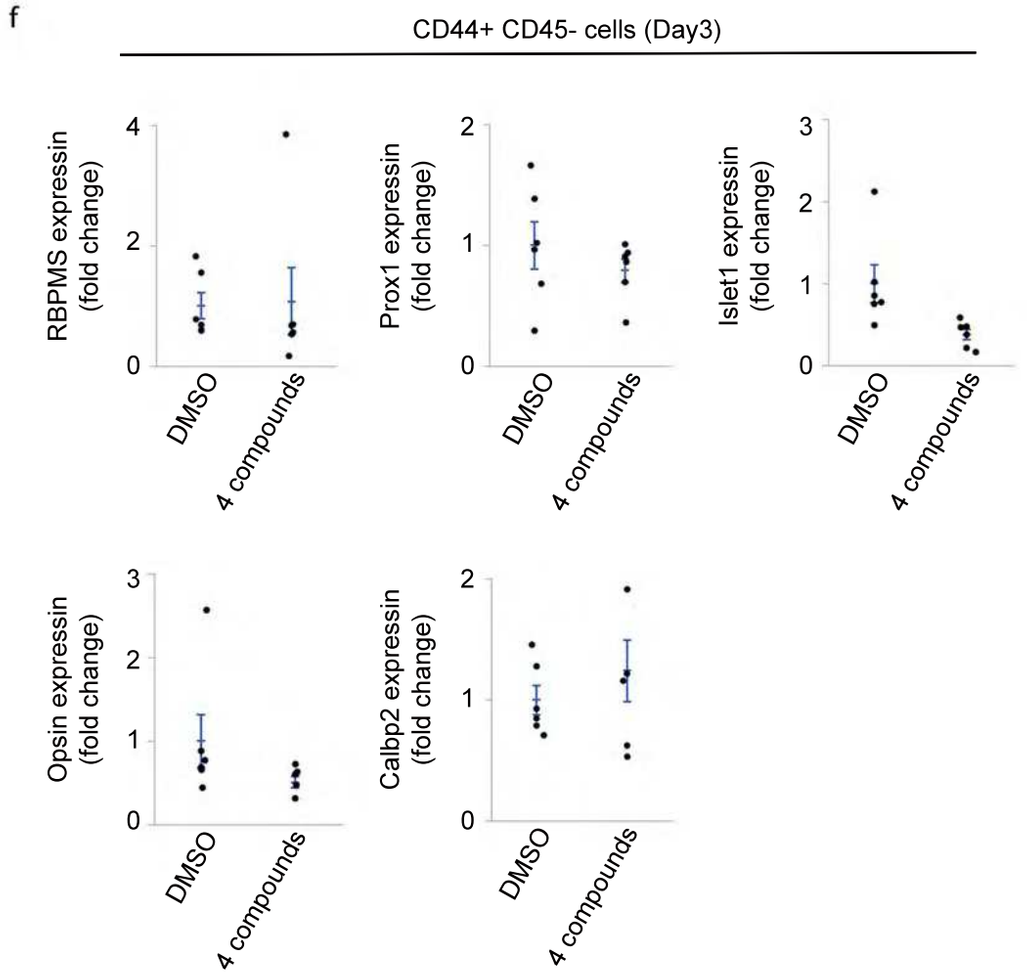
f
CD44+ CD45- cells (Day3)
RBPMS expressin
(fold change)
Prox1 expressin
(fold change)
Islet1 expressin
(fold change)
Opsin expressin
(fold change)
Calbp2 expressin
(fold change)
DMSO
4 compounds

Figure 2

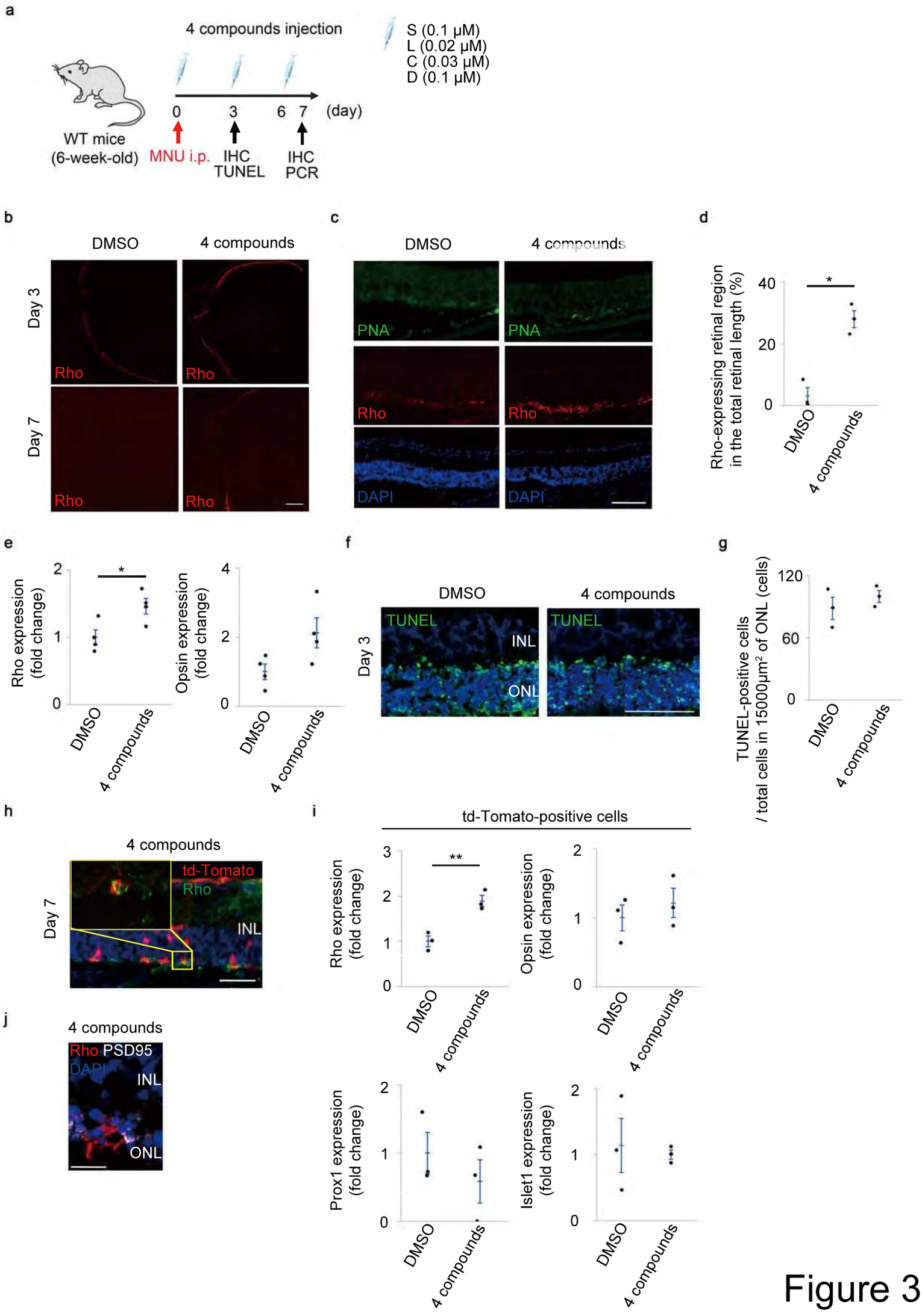
a
4 compounds injection
S (0.1 μM)
L (0.02 μM)
C (0.03 μM)
D (0.1 μM)
WT mice
(6-week-old)
MNU i.p.
IHC
TUNEL
IHC
PCR
0
3
6
7
(day)
b
DMSO
4 compounds
Day 3
Day 7
Rho
c
DMSO
4 compounds
PNA
Rho
DAPI
d
Rho-expressing retinal region
in the total retinal length (%)
DMSO
4 compounds
e
Rho expression
(fold change)
Opsin expression
(fold change)
f
DMSO
4 compounds
Day 3
TUNEL
INL
ONL
g
TUNEL-positive cells
/ total cells in 15000μm² of ONL (cells)
h
4 compounds
Day 7
td-Tomato
Rho
INL
i
td-Tomato-positive cells
Rho expression
(fold change)
Opsin expression
(fold change)
Prox1 expression
(fold change)
Islet1 expression
(fold change)
j
4 compounds
Rho PSD95
DAPI
INL
ONL

Figure 3

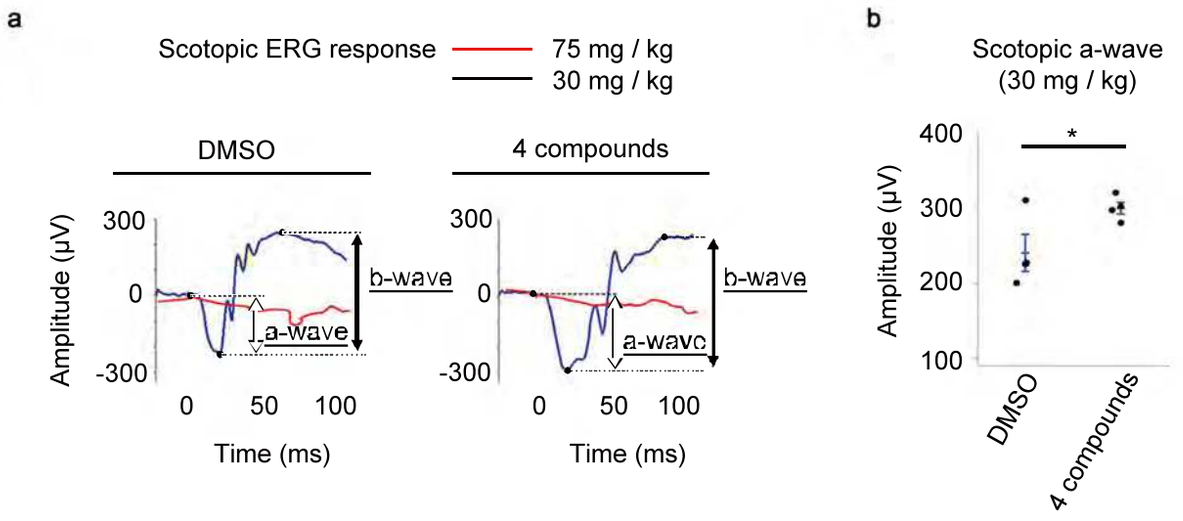
a
Scotopic ERG response
75 mg / kg
30 mg / kg
DMSO
4 compounds
Amplitude (μV)
300
0
-300
a-wave
b-wave
0
50
100
Time (ms)
b
Scotopic a-wave
(30 mg / kg)
400
300
200
100
*
DMSO
4 compounds

Figure 4

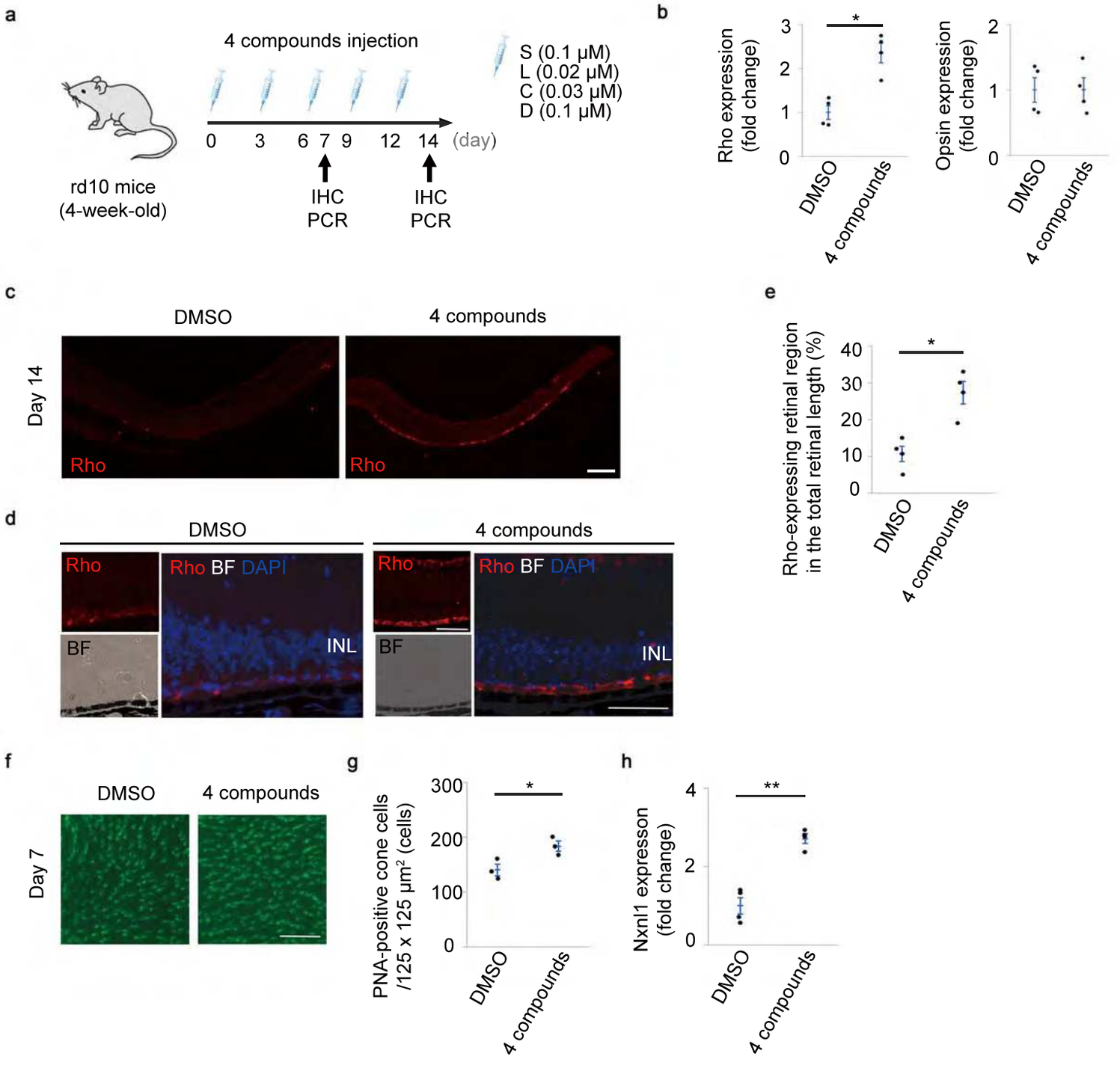
a
4 compounds injection
S (0.1 μM)
L (0.02 μM)
C (0.03 μM)
D (0.1 μM)
0 3 6 7 9 12 14 (day)
rd10 mice
(4-week-old)
IHC
PCR
IHC
PCR
b
Rho expression
(fold change)
Opsin expression
(fold change)
DMSO
4 compounds
c
DMSO
4 compounds
Day 14
Rho
d
Rho BF DAPI
BF
INL
e
Rho-expressing retinal region
in the total retinal length (%)
f
Day 7
g
PNA-positive cone cells
/125 x 125 μm² (cells)
h
Nxnl1 expresson
(fold change)

Figure 5

Supplementary Files

This is a list of supplementary files associated with this preprint. Click to download.

- supplementaryfile.pdf